4

Seismic Attributes in Hydrocarbon Reservoirs Detection and Characterization

4 Seismic Attributes in Hydrocarbon Reservoirs Detection and Characterization

Mohammed Farfour

National Company of Geophysics (ENAGEO), Boumerdès, Algeria.

Email: m84.farfour@gmail.com

Summary

Hydrocarbon-charged sediments detection and characterization is the main concern of petroleum explorers and producers. Over the past decades the Amplitude Variation with Offset (AVO) technique had proved to be a very successful tool in hydrocarbon identification and recognition. AVO attributes have been used particularly to extract information about the lithology (sand, shale, etc.) and fluid content of the subsurface. It unraveled successful discoveries in many sedimentary basins around the globe. The success was documented mainly in the Gulf of Mexico and analogous shallow unconsolidated rocks of tertiary age worldwide.

However, due to the fact that most of the hydrocarbon potential reserves in those basins and in easily explored areas have been discovered, the attention of the oil industry has been directed to enhance recovery from producing formations and exploring more difficult and complex environments (e.g. deep offshore, deep closely stacked thin bedding reservoirs, thin narrow and meandering reservoir channels, etc.). Thus, AVO attributes are insufficient for achieving the goals reached in earlier time. With the advent in seismic attributes technology, innovative seismic attributes appeared and proved to have potential in achieving information which used to be extracted using AVO. Of these innovative attributes, Spectral Decomposition (SD) proved to be a powerful tool in revealing subtle details that a

seismic broad band may burry. Over the last decades, numerous published works have discussed how this attribute can be used to differentiate both lateral and vertical lithologic and pore-fluid changes; as well as delineating stratigraphic traps and identifying subtle frequency variations caused by hydrocarbons from world different environments and geological settings.

The first section of this chapter focuses principally on the definition of seismic attributes and their applications in reservoir studies from the literature. In this context, AVO and SD attributes are introduced as direct hydrocarbon indicators (DHI), their successful implementations and limitations. Further aspect to this investigation discusses some real examples from different basins (Blackfoot, Canada; Boonsville field, South Texas).

4.1 Introduction

"Seismic Attributes" are defined as all of the measured, computed or implied quantities obtained from the seismic data. Therefore, this includes complex trace attributes, seismic event geometrical configurations, and their spatial and pre-stack variations. Attributes are generally computed from the seismic data represented in time, rather than in depth.

Attributes are related to the fundamental information in seismic data: time, amplitude, frequency, and attenuation. Note that many of the attributes in use are poststack, that is from the stacked and migrated data volume loaded on our workstations.

The prestack attributes are principally derived from amplitude variations with offset (AVO) measurements (Rutherford and Williams, 1989). This involves amplitude intercept, gradient, fluid factor (Smith and Guidlow, 1987; Fatti et al., 1994). Horizon attributes are extracted along a time slice or tracked horizon and

thus benefit from the precision of machine auto-trackers. Windowed attributes, on the other hand, use the sample values at, for example, 2 or 4 ms intervals. They may add up or average all the sample values to give a gross attribute, they may select one unique attribute value, or a distribution or trend in the attribute values over the window may be calculated. Time-derived attributes help to discern structural details. Amplitude-derived and frequency-derived attributes address problems of stratigraphy and reservoir properties. Amplitude attributes are here the most robust and useful, but frequency attributes may help reveal additional geologic layering (Brown, 2001). With the advent of the seismic attribute technology, great attention was drawn to frequency attribute them with amplitude attributes. One of the frequency attributes that gain popularity and wide use in industry is the spectral decomposition.

The spectral decomposition is an innovative seismic attribute used for reservoir imaging and interpretation technology originally developed and commercialized by BP, Apache Corp. and Landmark (Partyka et al., 1999). The technology utilizes a sequence of seismic frequency slices through an area of interest to create a suite of amplitude maps which can be selectively combined to yield much higher resolution images of reservoir boundaries, lithologic heterogeneities and interval thicknesses than traditional broad-band seismic displays (Burns and Street, 2005). In fact, over the last decade numerous published work discussed how this new attribute can be used to differentiate both lateral and vertical lithologic and pore-fluid changes (Burnett et al., 2003, Sinha et al., 2005 , Goloshubin et al., 2006, Chen et al., 2008 and Suarez et al., 2008); as well as how it can delineate stratigraphic traps and identify subtle frequency variations caused by hydrocarbons (Burnett et al., 2003, Castagna et al., 2003, Goloshubin et al., 2006, Miao et al., 2007). Moreover, in their study, Chapman et al. (2005) have extended the application of spectral decomposition analysis to AVO studies in the framework of the Rutherford and Williams AVO analyses

(Rutherford and Williams, 1989). Extensive modeling studies have been performed on the effects of tuning on the spectral characteristics, and these studies have been published in a series of companion papers by Odebeatu et al. (2006), Chapman et al. (2006) and Zhang et al. (2007); they suggested that the thin-layer tuning effect can be significant and is dependent on both offset as well as the ratio of the layer thickness over wavelength. However, dispersion/attenuation still modify the spectral characteristics caused by tuning and the tuning effect alone cannot cause the AVO anomalies brightening. Thus, the observed spectral variations are due to the combined effects of both tuning and dispersion/attenuation of seismic waves in porous sands.

While several studies in many different basins in the world demonstrated that AVO can lead to erroneous interpretation due to several geological conditions that can generate false anomalies (e.g. Loizou and Chen 2012, Forrest et al., 2010, Roden et al., 2005 among others), a growing number of surveys over different oil and gas fields throughout the world have established the presence of spectral anomalies with a high degree of correlation to the location of hydrocarbon reservoirs (e.g. Loizou and Chen 2012; Burnett et al., 2003, Castagna et al., 2003, Goloshubin et al., 2006, Miao et al., 2007, Yoon and Farfour, 2012, Farfour et al., 2012).

4.2 Amplitude Variation with Offset (AVO) in Reservoir Characterization

Amplitude variations with offset techniques are used by exploration, development, and production teams to assist hydrocarbon identification in clastic depositional settings.

While exploration groups tend to use AVO attributes for detection and risk

quantification, exploitation and production groups use AVO attributes for reservoir characterization and even fluid-front monitoring (Ross, 2002).

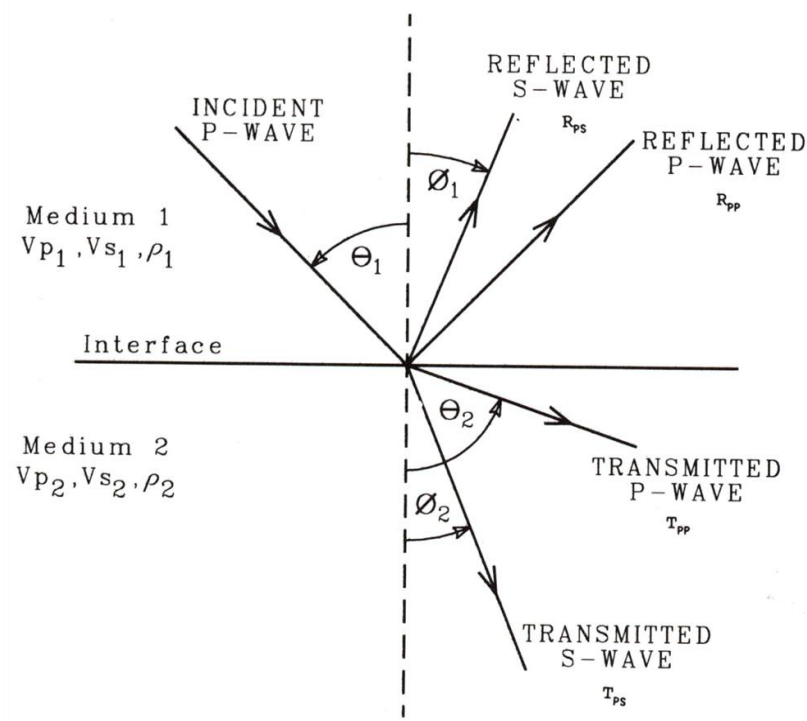

Figure 1. *Reflection and transmission at an interface between two infinite elastic half-spaces for an incident P-wave (Castagna and Backus, 1993).*

The main idea behind AVO attributes is the linearized approximations of the Zoeppritz (1919) equations. The simplified expression is used in AVO attributes computation and inversion to extract petrophysical parameters, such as P-wave and S-wave impedance and velocity, elastic moduli resulted from energy partitioned and wave conversion (Figure 1), and then infer the fluid content from cross-plots of these parameters.

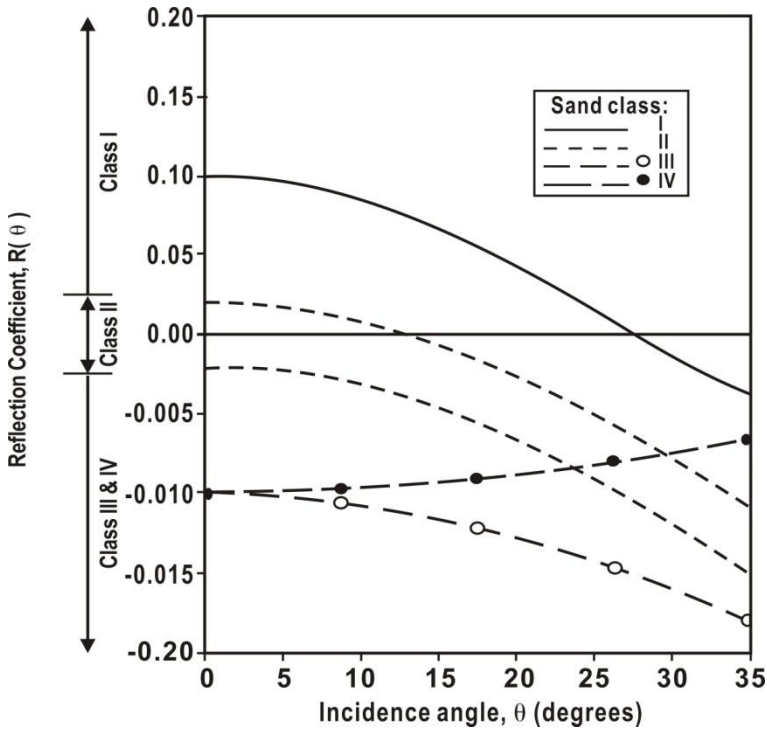

Figure 2. *Plan wave reflection coefficients at the top of each Rutherford and Figure 2. William (1989) classification of gas sands. In addition to Class IV of Castagna et al. (1998).*

Most common AVO attributes are AVO intercept, gradient, curvature and fluid factor (Smith and Guidlow, 1987). Figure 2 shows the Castagna et al.'s (1998) classification of AVO types. The Class I, II and III curves show the Rutherford and Williams (1989) classification for gas sands. Note that this classification is based only on the normal-incidence reflection coefficient (intercept A). Class I sands are high impedance relative to the overlying shales and give positive AVO intercept (A) and negative AVO gradient (B). Class II sands have low normal incidence reflectivity (small impedance contrast). Class III sands are lower impedance than the overlying shales, and exhibit increasing reflection magnitude with offset (negative AVO intercept, A, and negative AVO gradient, B). Class IV

was introduced by Castagna et al. (1998) for the case where initially negative reflection coefficients become more positive with increasing offset (negative intercept, A, and positive gradient B). Phase reversals may be associated with Class I AVO in far offsets, and may occur for Class II in the near to middle offsets (Loizou et al., 2008).

4.3 Interpretation of AVO Data

AVO has many applications in oil industry. Gas-sand detection is the most promising application of AVO analysis due to the characteristically low V_p/V_s of gas sands which differentiate them from other low impedance layers such as coals and porous brine sands (Rutherford and Williams, 1989). Ito et al. (1979) and others, show that AVO can be used in an enhanced oil recovery and the effect of steam on rock V_p/V_s is very similar to the effect of natural gas. Whereas Tsingas and Kanasewich (1991) showed that AVO can be very effective for monitoring steam flooding. Additionally, under favorable circumstances oil sands can exhibit V_p/V_s ratios about half-way between brine and gas (Gassaway, 1984; and Chiburis, 1987). Furthermore, it has been found that inspection of V_p versus V_s trend curves for sandstones, shales, limestones, and dolomites, reveals that lithology discrimination is the most robust at higher velocities where sandstones have low V_p/V_s (1.5-1.6) and the other lithologies have higher V_p/V_s (1.7-2.0) (Castagna et al., 1993).

Note that AVO can be used also to detect the porosity in carbonates. Given the highly variable pore structure of carbonates, it is difficult to make generalizations regarding expected AVO response without a local calibration. V_p/V_s is usually insensitive to porosity and pore fluid content (with the sometimes important exception of unconsolidated carbonate sands or lithified

carbonates with flat pores or microfractures). For the vuggy porosity dominated by equant (spherical) pores, density may be the parameter which is most sensitive to porosity and pore fluid content; density becomes even more important when the rock has a variable clay content. In these cases, Shuey's third coefficient (C) may be required to separate velocity and density contrasts.

4.4 Limitations and Pitfalls of AVO

A major uncertainty in the interpretation and risk analysis of seismic amplitude anomalies is the presence of a pitfall. An anomaly can be caused by:

- A reflectivity from the top of a clean, high-porosity wet sand.
- A low-saturation gas sand (can have positive AVO and downdip conformance similar to commercial gas sand).
- No reservoir (low-impedance shale, a gas-filled silt, or a marl).
- Tight sands.
- Top hard pressures.
- Seismic processing artifacts.
- Salt, volcanics, carbonates (polarity issue).
- CO2.
- Tuning effect, especially AVO tuning.
- Lateral lithology or thickness change.

It is important to keep in mind that to interpret AVO results, the interpreter must have a good understanding of how various geologic situations will manifest themselves in the prestack domain. There are many variables that change the

prestack response. Both the rock physics and the seismic response influence the prestack response.

It is also important to remember that amplitude variation with offset anomalies can arise whitout having nothing to do with geology. It is just a result of the propagation of the seismic wavefield and factors that affect the amplitudes while traveling to deeper formations (Downton et al. 2000).

The accuracy of the AVO and geologic predictions become subject to how suitable the processing deals with these factors. Thus, the data must be processed in an AVO friendly fashion. Furthermore, depth trend can play a major complicating role in the behaviour of amplitude. That is, elastic properties of rocks are strongly influenced by local geologic trends and can change markedly even within a sedimentary basin. Critical geologic factors that control elastic properties can be either related to a depositional environment or a burial history. The knowledge about the expected change in seismic response, as a function of depositional or compactional trends, will increase the ability to predict hydrocarbons, especially in areas with little or no well log information. In general, seismic velocities and densities of siliciclastic sedimentary rocks will increase with depth due to the compaction and the porosity reduction and the seismic signature can be very different from one depth to another due to different compaction trends for different lithologies. Therefore, it is necessary to include depth as a parameter when we use AVO analysis to predict lithology and pore fluids from seismic data (Avseth et al., 2003).

4.5 Spectral Decomposition in Reservoir Characterization

The standard seismic data processing flow involves transforming a set of CDP gathers into a stacked section. The assumption behind stacking is that the

amplitudes on the gather do not show much variation, so that stacking can be considered as simply a noise cancellation technique.

Post-stack seismic attributes have come a long way since their introduction in the early 1970s and have become an integral part of seismic interpretation projects. Today, they are being widely used for the lithological and the petrophysical prediction of reservoirs and various methodologies have been developed for their application to a broader hydrocarbon exploration and a development decision making. Beginning with the digital recording of seismic data in the early 1960s and the ensuing bright spot analysis, the 1970s saw the introduction of complex trace attributes and seismic inversion along with their color displays. Since then, several gained popularity amongst interpreters (trace envelop or instantaneous amplitude, frequency, phase, attributes derivatives, etc.). This was followed by the development of other more advanced attributes. One of these attributes is decomposing a seismic signal band into constituent frequencies (Chopra and Marfurt, 2007).

The concept behind Spectral decomposition is that seismic broadband can be spectrally decomposed into constituent frequencies. The process involves the following steps: decompose the seismogram into its constituent wavelets using wavelet transform (Sinha et al., 2005) or small time windows using Short Time Window Fourier Transform (Partyka et al., 1999). Sum the Fourier spectra of the individual wavelets in the time frequency domain and sort them to produce iso-frequency cubes, section, time slices, and horizon slices (Castagna et al., 2003). This decomposition proved to be a powerful tool in revealing subtle details that seismic broad band may burry. Over the last decades, numerous published works have discussed how this attribute can be used to differentiate both lateral and vertical lithologic and pore-fluid changes; as well as delineating stratigraphic traps and identifying subtle frequency variations caused by hydrocarbons.

4.6 Short Window Discrete Fourier Transform (Transform Using Constant Size Windows)

For a non-stationary signal such as a seismogram, the frequency content changes with time. The amplitude spectrum of the Fourier transform indicates the presence of different frequencies but does not show temporal distribution of these frequencies. If we assume that the signal through a small window of time is stationary, then its Fourier transform or Short Time window Fourier Transform (STFT) provides us with the frequency content of the signal in that time period. By shifting this time window appropriately, the frequency content of the signal is extracted and a 2-D representation of frequencies versus time is produced (Chakraborty and Okaya, 1995).

The conventional spectral decomposition is usually performed using the short window discrete Fourier transform (SWDFT). Partyka *et al.* (1999) proposed the application of the SWDFT to generate common frequency cubes. They first selected a data analysis window containing stratigraphic features of interest. The next step is to transform the time-domain data to the frequency domain using the SWDFT. After a spectral balancing, they viewed the decomposed common frequency horizon slices to identify textures and geological patterns.

The equation for the short window discrete Fourier transform can be written as (Mallat, 1989).

$$U_{STFT}(\tau, f) = \frac{1}{\sqrt{2\pi}} \int u(t) w(t-\tau) e^{-j\,2\pi f t}\, dt \tag{1}$$

where $u(t)$ is the time domain seismic data, τ is the center time of the window function $w(t-\tau)$, f is the frequency, and $U_{STFT}(\tau, f)$ is the time-frequency function.

The defined window $w(t-\tau)$ can be either a tapered or untapered rectangular window (boxcar), Gaussian window, Hamming window, or Hanning window (Mallat, 1989).

Partyka et al. (1999) use a tapered rectangular window, while Mallat (1989) uses a Gaussian window of the form:

$$w(t-\tau) = e^{-\sigma^2(t-\tau)^2} \tag{2}$$

where σ is a constant value controlling the window size, with larger values of σ resulting in smaller time windows.

Traditionally, the Fast Fourier transform (FFT) has limited vertical resolution because the seismogram must be windowed.

The spectral energy is distributed in time over the length of the window, thereby limiting resolution. If the time window is too short, the spectrum is convolved with the transfer function of the window, and the frequency localization is lost (i.e., the frequency spectrum is smeared). This can be mitigated to some extent by tapering the window, but it is obviously preferable to avoid windowing altogether. Another disadvantage of a short window is that side lobes of arrivals appear as distinct events in the time-frequency analysis. If the time window is lengthened to improve frequency resolution, multiple events in the window will introduce notches that dominate the spectrum. Long windows thus make it very difficult to ascertain the spectral properties of individual events. As an alternative solution, Continuous Wavelet Transform (CWT) can be used. The CWT method does not require preselecting a window length and does not have a fixed time-frequency resolution over the time frequency space. CWT uses dilation and translation of a wavelet to produce a time-scale map. A single scale encompasses a frequency band and is inversely proportional to the time support of the dilated wavelet.

4.7 Spectral Decomposition Using Continuous Wavelet Transform

A wavelet transform (WT) is also a technique to decompose a signal to identify its frequency distribution through time. This technique differs from the Short Time window Fourier Transform (STFT) in that while an STFT uses a fixed size time window, a wavelet transform uses a variable window size.

The continuous wavelet transform (CWT) is an example of the WT technique. It was first introduced in Morlet et al. (1982) and Goupillaud et al. (1984), but received full attention of the signal processing community when Daubechies (1988) and Mallat (1989) established connections of the WT to discrete signal processing.

The main advantage of using a CWT over a STFT in addition to that mentioned previously is that the CWT has a good frequency resolution for low frequencies and a good time resolution for higher frequencies (Chakraborty and Okaya, 1995 and Castagna et al., 2003). In the CWT, wavelets dilate in such a way that the time support changes for different frequencies. A smaller time support increases the frequency support, which shifts toward higher frequencies. Similarly, a larger time support decreases the frequency support, which shifts toward lower frequencies. Thus, when the time resolution increases, the frequency resolution decreases, and vice versa (Mallat, 2009).

A wavelet is defined as a function $\psi(t) \in L^2$ (IR) with a zero mean, localized in both time and frequency. By dilating and translating this wavelet $\psi(t)$, we produce a family of wavelets

$$\psi_{\sigma,\tau}(t) = \frac{1}{\sqrt{\sigma}}\psi\left(\frac{t-\tau}{\sigma}\right) \tag{3}$$

where σ >0 is the dilation parameter or scale and τ ∈IR is translation parameter. Note that the wavelet is normalized such that the L^2- norm $|\psi|$ is equal to unity.

The CWT is defined mathematically as the inner product of the family of wavelets ψσ, τ with the signal s (t).

$$S_w(\sigma,\tau) = \int_{-\infty}^{\infty} s(t)\left(\frac{1}{\sqrt{\sigma}}\right)\bar{\psi}\left(\frac{t-\tau}{\sigma}\right)dt \quad (4)$$

where $\bar{\psi}$ is the complex conjugate of ψ and S_w is the time scale map (scalogram) (Sinha et al., 2005).

Note that CWT also suffers from some disadvantages in that the wavelets utilized must be orthogonal. Furthermore, experience has shown that a DFT with a Gaussian window of appropriate length produces almost the same result as a CWT with a Morlet wavelet.

4.8 Attributes Analysis and Application on Field Data

4.8.1 Case Study 1: Spectral Decomposition in Imaging Challenging Reservoirs

The reservoir system I study here is the Bend Conglomerate, a productive series of gas reservoirs composed of Middle Pennsylvanian fluvio-deltaic clastics. In the previous study by Hardage et al.(1996a), seismic instantaneous attributes were used to define the Upper and Lower Caddo reservoir facies distribution in Boonsville field, North Central Texas. The authors treated each reservoir with a different attribute. They used an instantaneous frequency to map Lower Caddo and an averaged instantaneous amplitude for Upper Caddo imaging. The attributes could indicate some of Lower Caddo but failed to map Upper Caddo without ambiguity. Note that hydrocarbons sand in this field are characterized by

high impedance compared to their background (similar to AVO Class I gas sand), thus, the amplitude of the reservoir was dimming at stack section. Thus, the amplitude attributes would not be helpful in such cases. I then use Time Frequency Continuous Wavelet Transform to study the spectral-decomposition response to stratigraphic features of the Caddo sequence. Spectrally decomposing the data successfully resolves both reservoir distributions and delivers facies extensions that correlate with well data information. Moreover, by spectrally decomposing individual traces from different zones, it inferred that the misleading non-reservoir facies apparent in Hardage et al. (1996a)'s attributes maps are characterized by frequency responses different than the Caddo reservoirs facies.

Geological Setting

Boonsville gas field is located in the Fort Worth Basin of North-Central Texas (Figure 3). The reservoir system I study is the Bend Conglomerate, a productive series of gas reservoirs composed of Middle Pennsylvanian fluvio-deltaic clastics 900 to 1300 ft (275 to 400 m) thick in our project area, with the base of the interval being a little less than 6000 ft (1830 m) deep. I focus particularly on the Caddo interval which is one of the most productive in the area.

The Caddo contains two discrete sandstone bodies, one occurring within a Lower Caddo between MFS80 and Caddo limestone and one in an Upper Caddo between MFS90 and Caddo limestone (Figure 4).

Note that most of the Caddo production in our study area is oil, however, significant gas reserves have been found in some Upper Caddo wells that are located structurally downdip relative to the Lower Caddo oil accumulations, indicating that the two units are physically separate reservoir compartments.

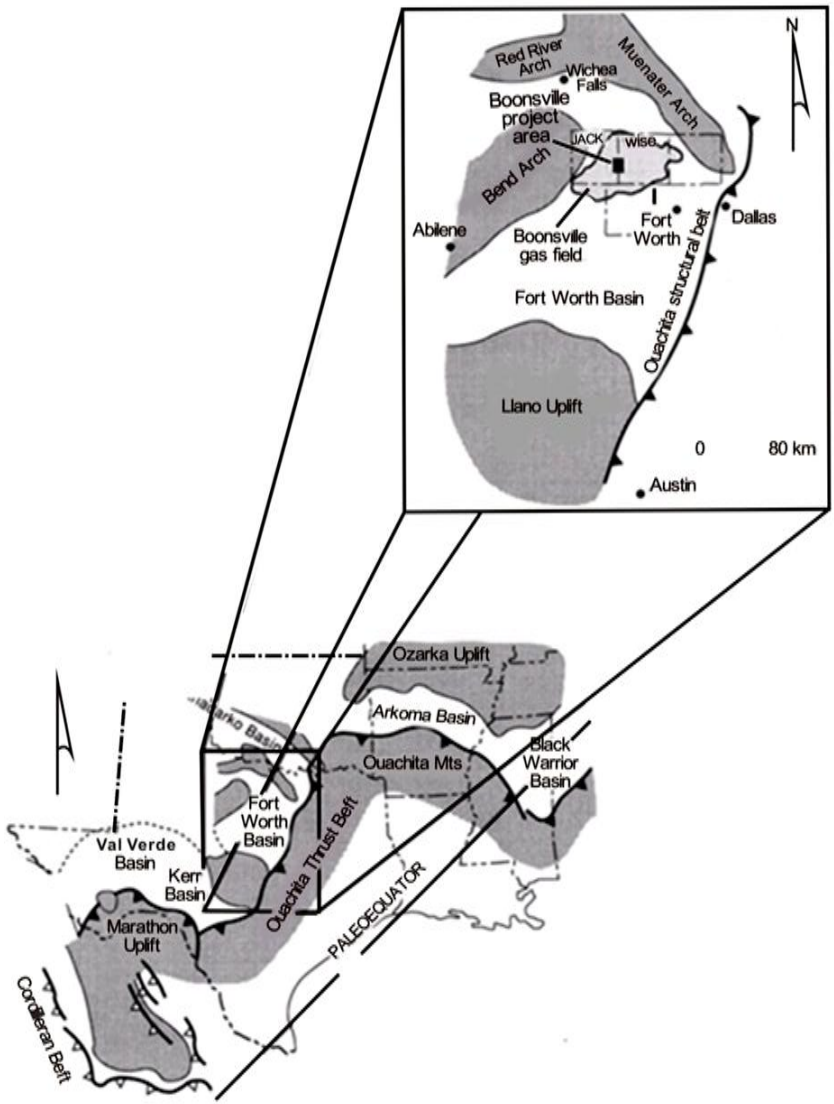

Figure 3. *Boonsville project area. The solid rectangle on the Wise-Jack county line designates the area where 3-D seismic data where gathered and where most of the research work was performed (From Hardage et al., 1996a).*

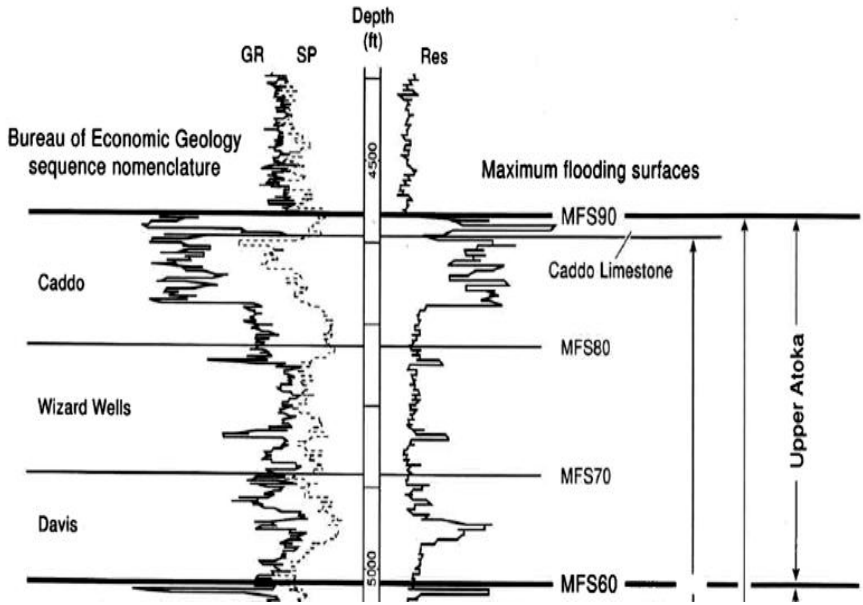

Figure 4. *Bend conglomerate genetic sequence in Boonsville field identified on Gamma Ray (GR), Spontaneous Potential (SP) and Resistivity (Res) logs (From Hardage et al., 1996b).*

Methodology

The primary seismic imaging objective was to delineate the Lower and Upper Caddo reservoir boundaries and to distinguish sand-fill from limestone-fill. Additionally, very dense tracking application was used to reduce errors stemming from auto-tracking. The mapping technique enabled me to track horizons rapidly and safely. Note that both reservoirs in addition to the thin bed limestone that separates them do not exceed 30ms time interval starting from the tracked horizon. Figure 5 displays a time window spanning both Caddo reservoirs.

Seismic attributes then were calculated and performed profound analysis over the time correlating to the reservoirs. After that the spectral-decomposition response to different fills at different frequencies has been studied carefully. Each frequency component was expected to help in the interpretation of subtle details

of the stratigraphic framework of the reservoir.

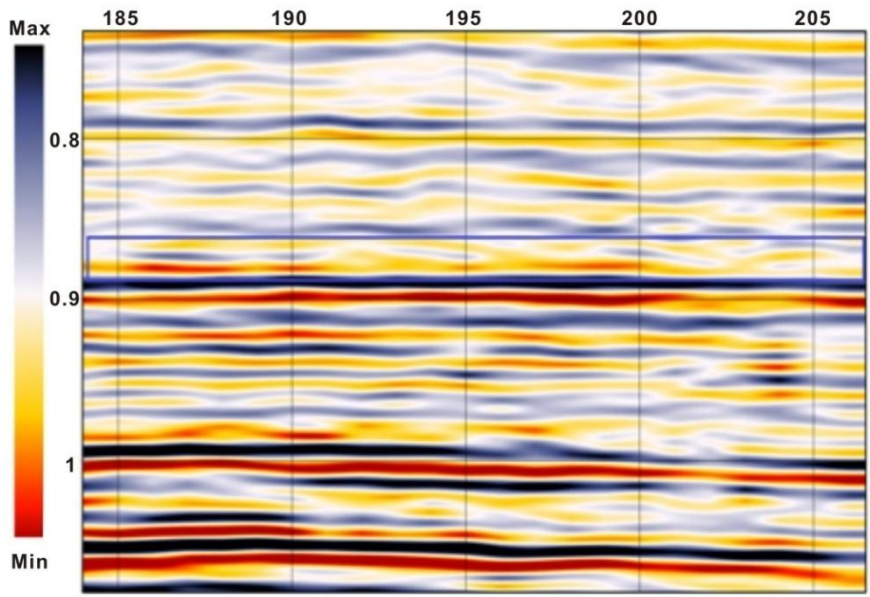

Figure 5. *Seismic line passing across the targeted reservoirs. Note that the two reservoirs and limestone bed fall within the time interval bounded by the blue rectangle.*

Results and Discussion

From the previous work, results obtained by Hardage et al. (1996a) showed that some areas of the Lower Caddo reservoir can be clearly pronounced using seismic attributes.

In Figure 6, the increase in the instantaneous frequency observed around the producing wells from Lower Caddo, implied that the reservoir is very thin at this area. This was supported by well data information which showed that the net reservoir thickness in this area is about 20 to 30ft.

While the averaged instantaneous frequency did predict the Lower Caddo and shows results that are somewhat consistent with well based maps, the averaged

instantaneous amplitude could not predict reliably the Upper Caddo reservoir facies distribution (Hardage et al., 1996a). That is, Figure 7 shows that the Upper Caddo reservoir is present in certain wells in which well data demonstrated that the Upper Caddo sequence is dominated by two thin, non productive limestone units rather than the productive valley-fill sandstone reservoir. These two closely spaced limestone beds generate destructive amplitude dimming, similar to that occurs for valley fill sandstone reservoir facies. Thus, the attribute was found not an unambiguous indicator of the Lower Caddo reservoir distribution.

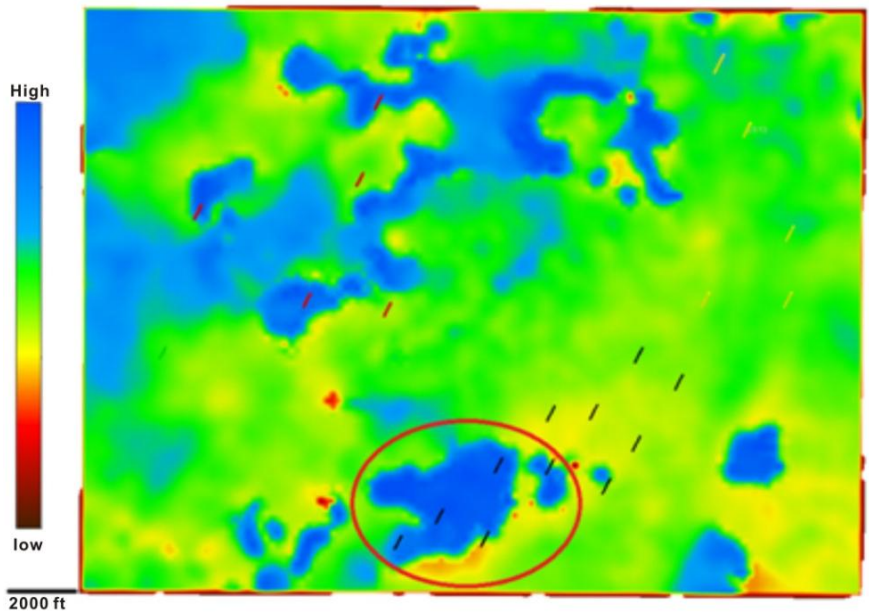

Figure 6. *Average instantaneous seismic frequency calculated within the Lower Caddo sequence. The map is found correlating with the Lower Caddo net reservoir sandstone map. Wells in black are producing from Lower Caddo while wells in yellow are from Upper Caddo. High frequency in the Lower Caddo zone is found coinciding with the net reservoir (red circle).*

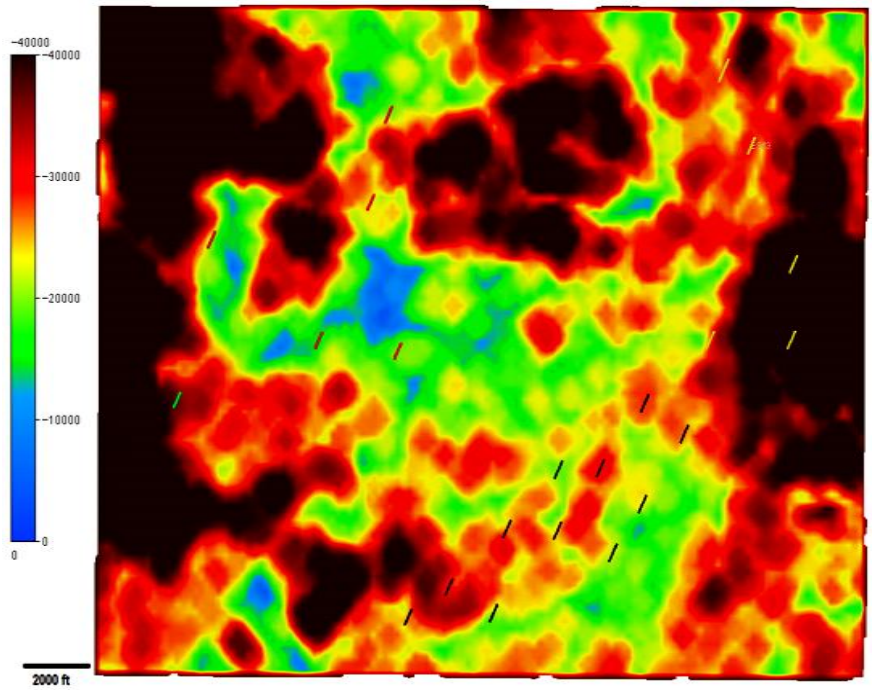

Figure 7. *Map of seismic amplitude attribute calculated within the Upper Caddo sequence. Blue and green amplitude zones were interpreted as producing zones. Well data implied that most of these zones are non-producing limestone zones. Wells in black are producing from Lower Caddo while wells in yellow are from Upper Caddo. Wells in red are producing from other intervals.*

We have expected that spectrally decomposing the data may help solve this problem. We thus have performed wavelet based spectral decomposition to the data. For this decomposition a Mexican hat wavelet was found to be the best in terms of a lateral frequency and vertical time resolutions. Figure 8 shows how clearly the Mexican hat wavelet decomposes the seismic trace into sub-frequencies compared to Gaussian and Mallat wavelets. Several frequencies have been calculated for the carefully tracked Caddo horizon. At 50 Hz the reservoir horizon frequency amplitude showed a very similar trend to the one that was observed in the instantaneous frequency map in Hardage et al. (1996a).

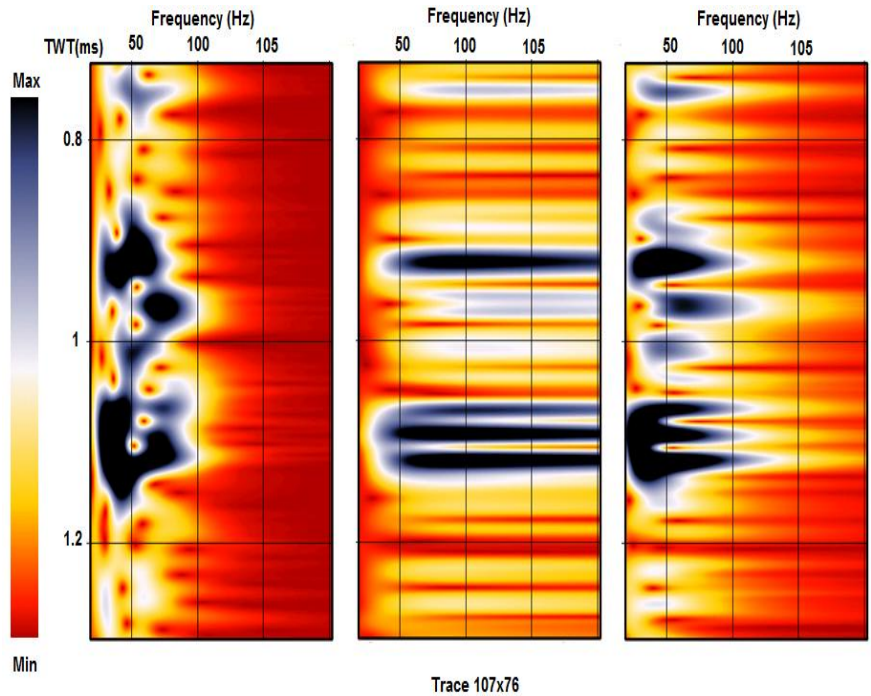

Figure 8. *Spectrally decomposing seismic trace a) using Mallat wavelet, b) using Gaussian wavelet and c) using Mexican hat wavelet. Note how Mexican hat yields clear spectral response with higher vertical resolution than Mallat wavelet and higher lateral resolution than the Gaussian wavelet.*

Referring to Figure 9, the 50Hz frequency image, surprisingly, could map not only the Lower Caddo but also the Upper Caddo as it is shown in the northeastern part. The reason that the two reservoirs were seen in the same horizon frequency image is due to the fact that the reservoirs are thin (below tuning) and so close vertically that their images can be seen in one horizon. Both reservoir intervals are located within a time window not exceeding 30ms. In such situations, geologic features or at least most of them, can be seen on more than one closely spaced horizon. It is up to the interpreter to choose the interval where the feature analyzed is best resolved (Roksandic, 1995).

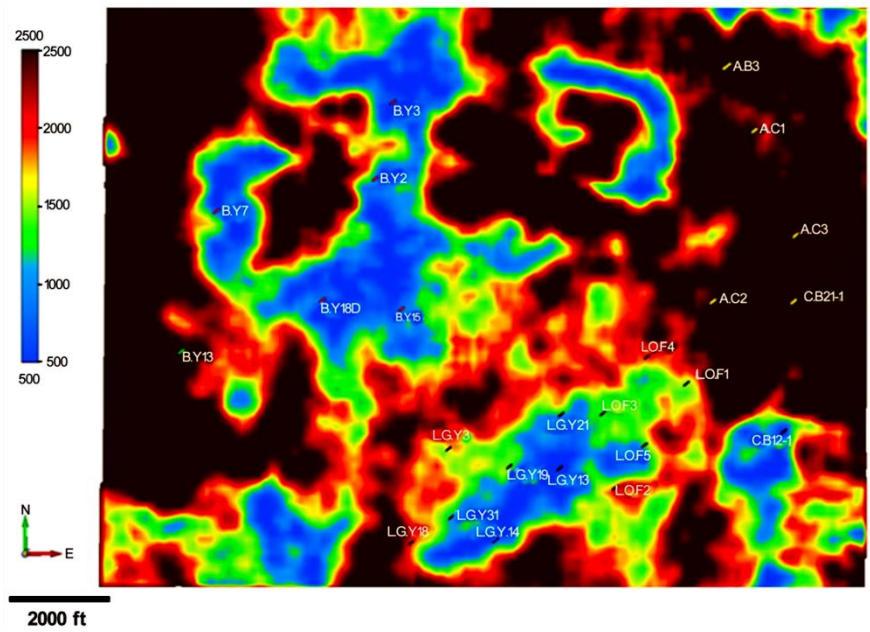

Figure 9. *50Hz horizon shows Lower and Upper Caddo reservoirs distributions. Note that all Lower Caddo producing wells (in black) lie in low amplitude, while Upper Caddo producing wells (in yellow) fall in high amplitude.*

Furthermore, it is easy to notice that all producing wells (in black) from the Upper Caddo reservoir are characterized by a low frequency amplitude trending northeastward; while the wells producing from Upper Caddo (yellow) are associated with a high spectrum amplitude. I propose the following interpretation for these amplitude changes. The high amplitude anomaly shown in the zone encompassing Upper Caddo wells can be attributed to the following fact. In presence of hydrocarbons, encasing formations selectively reflect some particular frequencies and not others. Thus, at 50Hz in particular the Upper Caddo reservoir is significantly brighter than other adjacent formations. One can attribute this high amplitude to the thin bed effect and the hydrocarbon charge. The latter makes the reservoir reflection coefficients larger than those of other surrounding areas, and the thin-bed tuning effect preferentially reflects 50Hz

making the 50Hz image brighter than other frequencies.

In the contrary, at the lower Caddo reservoir, I have noticed a very low amplitude at this frequency (50Hz) relative to the one seen in elsewhere. Note that the anomalously low frequency trend is found to be matching with Lower Caddo reservoir distribution and geographic bounds implied by well control. This frequency response is considered associated with high attenuation that high frequencies have encountered while traveling hydrocarbon reservoirs. Note that although reservoirs are so close, their frequency responses are very different. This can be partly associated to their thicknesses as thickness is one of the key factors controlling reservoirs spectral decomposition responses (Chen et al., 2008).

Note that both frequency behaviors are well documented in Castagna et al. (2003), Burnett et al. (2003) and Chen et al. (2008).

It is important to note that there exist other areas, where neither Caddo's Lower nor Upper reservoir was penetrated, are showing somewhat similar frequency responses to those illustrated above. Indeed, the low spectrum amplitude anomaly passing through the wells B.Y2, B.Y3 and B.Y18D was found similar to that of Lower Caddo. Thus, the anomalously low spectrum amplitude is not a reliable diagnostic of the hydrocarbon charged Caddo formation. To remove this ambiguity, I have extracted traces at producing well locations and traces at non producing well zones for a more detailed spectral analysis and calibration. Figure 10 and 11 respectively, depict the spectrum decomposition of single traces from the Lower Caddo producing wells (I.G.Y13, 21 and 31) and traces from wells positioned in the limestone zone (B.Y3, 18D and 15). It should be ensured that the information in individual traces come from consistently gridded small zones (110ft x 110ft bin size). Frequency images from these traces revealed that frequency behaviors of hydrocarbon producing zones and limestone dominated zone are different although they appear similar in the overall frequency response map.

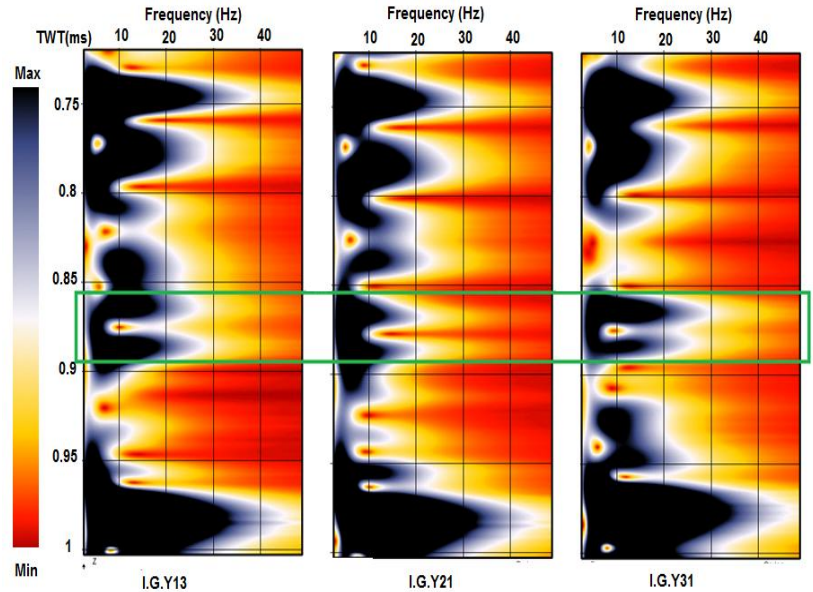

Figure 10. *Frequency response at the lower Caddo reservoir followed by low frequency immediately below the reservoir interval.*

It can readily be seen that traces from lower Caddo show that high frequencies are present but faced a severe attenuation exactly at the reservoir location. The attenuated frequencies are followed by a low frequency immediately below the reservoir interval. On the other hand, in the traces from the non producing zone, these high frequencies were almost absent and this is followed by high frequencies presence instead, immediately below the reservoir interval (Figure 11).

This low frequency presence is commonly associated with hydrocarbon reservoirs where the thickness is not sufficient to result in significant attenuation (Castagna et al., 2003; Castagna and Sun, 2006).

Thus, the decomposition provides a very clear indication to separate non producing limestone beds from hydrocarbon encasing formations. As a result, by calibrating frequency responses with geology and engineering data, a

discrimination became straightforward. It is important to note that our interpretation is consistent with a more recent Caddo sequence depositional model derived from seismic and well data by Xie et al. (2004). See Figure 12.

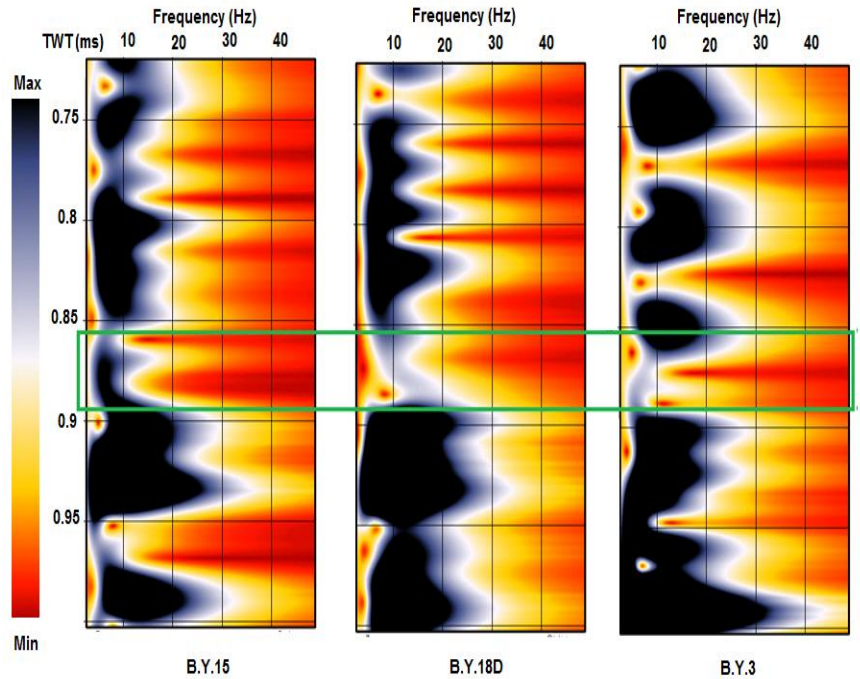

Figure 11. *A non-producing reservoir frequency response. Note that high frequencies previously observed are almost absent at the reservoir interval (green). A high frequency increase is observed immediately below the zone of study.*

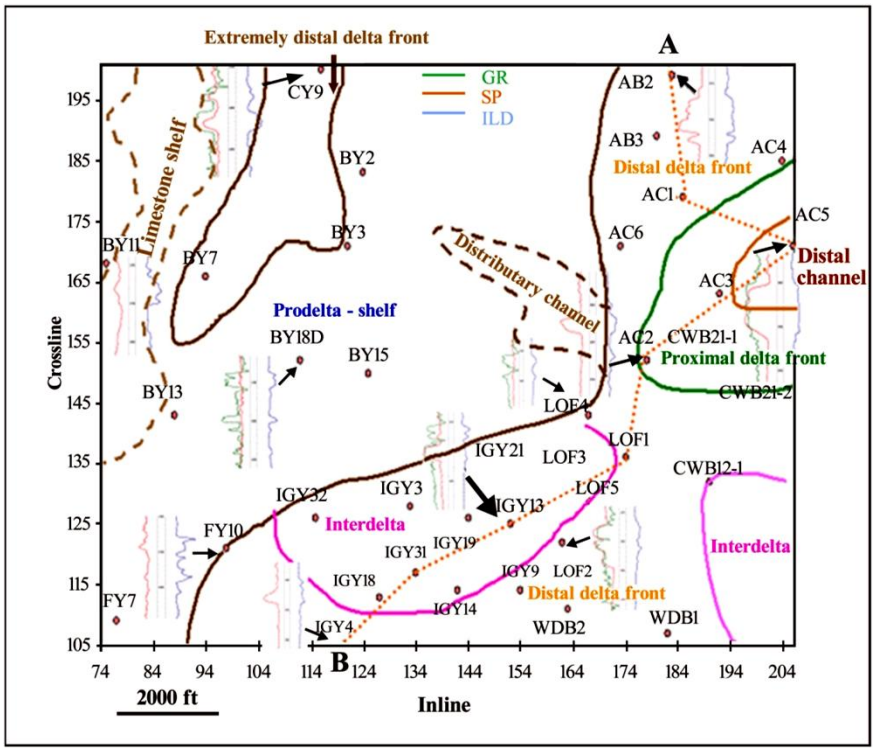

Figure 12. *Representative well log trends and depositional sub-facies of the Caddo sequence based on the well data; the possible limestone shelf and distributary channel based on the seismic inversion (From Xie et al., 2004).*

This study presents an example among many other successful applications of a spectral decomposition in a hydrocarbon reservoirs identification and characterization.

The spectral decomposition reveals successfully stratigraphic information of two reservoirs separated by a very thin bed limestone.

The overall frequency responses of different zones were not a so reliable indicator to discriminate a hydrocarbon producing sand from non producing zones. The investigation of individual traces frequency responses was investigated to remove the ambiguity.

The results obtained from the decomposition are very well consistent with geology and engineering information. Thus, the study demonstrates how seismic attributes once are best integrated and calibrated with engineering data can extract subtle features about reservoirs that may not be easy to achieve otherwise.

4.8.2 Case Study 2: Seismic Attributes in Illuminating a Thin Sand Channel Reservoir

The Amplitude variation with offset (AVO) analyses have proved to be a robust indicator of hydrocarbons in the Tertiary basin-floor fan plays offshore Angola and in Pliocene gas sand of Gulf of Mexico in addition to other comparable plays worldwide (for examples of AVO success studies in West Africa and Gulf of Mexico see Alexander et al., 2001, Castagna and Smith, 1994, and Rutherford and Williams, 1989). This success is based on the fact that gas-bearing sediments will exhibit seismic-reflection amplitudes that are anomalously higher than the surrounding reflections. There are, however, several other combinations of geological conditions whose seismic reflectivity signature can give rise to false large amplitudes such as high porosity, tuning effects, overpressured shales, Fizz water and others (see Han and Batzle, 2002 and Young and Tatham, 2007). This fact led to costly failures in many worldwide plays as well (e.g. Loizou et al., 2008; Forrest et al., 2010). Therefore, the need for techniques having the potential to reduce the risk resulting from false AVO anomaly has become a necessity.

Over the years and from various lessons that geophysicists have learned from the history of AVO, numerous advanced techniques have been incorporated to aid AVO analyses and became a routine application. The AVO fluid inversion (Hampson et al., 2004), AVO inversion (Hampson et al., 2005), elastic inversion (Connolly, 1999), extended elastic inversion (Whitcombe et al., 2002) and

spectral decomposition (Partyka et al., 1999; Chapman et al., 2005; Welsh et al., 2008) are examples amongst other applications widely used in this direction.

In this study, I use Short Window Fourier Transform to study the spectral decomposition response to reservoir fluid from western Canada. The geophysical interpretation of compressional PP seismic data resulted in the definition of the Glauconitic incised-valley width extent, and in the mapping of the Upper incised-valleys. However, the nature of the fill within the incised-valleys remains unknown. In an effort to discriminate lithology and to detect fluid, the AVO analyses of the PP-data were published by Dufour et al., (1998, 2002) and Margrave et al. (1998). A strong AVO response conforms to Class III AVO response of Rutherford and Williams (1989), was observed at the top of the porous sandstone in the upper valley, whereas the shale in the upper valley had a very different AVO response. The spectral decomposition run on post-stack data did confirm the information derived from the AVO analysis. Moreover, it did reveal also attenuations caused by the hydrocarbons along the channel.

AVO Inversion and LMR Extraction

The goal of the pre-stack seismic inversion is to obtain reliable estimates of P-wave velocity (Vp), S-wave velocity (Vs), and density (ρ) in order to predict the fluid and lithology properties of the subsurface of the earth. Whereas, the LMR (Lambda-Mu-Rho) technique is an AVO inversion, in which the prestack seismic CMP gathers are inverted to extract data volumes of Lamé's elastic rock parameters (λ and μ) combined with density (ρ), in the form $\lambda\rho$ and $\mu\rho$. Goodway et al. (1997) suggested that λ is the most sensitive fluid indicator. This parameter is normally embedded in the compressional velocity (Vp) and both λ and Vp take on low values for gas-saturated sands. Gas is very compressible and thus low values of $\lambda\rho$ are good indicators of gas saturated formations. The rigidity term $\mu\rho$ is considered the matrix indicator, as μ is insensitive to saturating fluids. In theory,

sand will have a high value of μρ because the dominant mineral in the sand matrix, quartz, has a higher rigidity than clay minerals. The combination of low λρ and high μρ, therefore, suggests a gas saturated sandstone, while higher λρ and lower μρ can be an indicator of shale presence. This technique is very powerful and provides a direct geological meaningful information about targets, however it does have some problems when prestack data quality is not so good (e.g. Young and Tatham, 2007).

Geological Setting

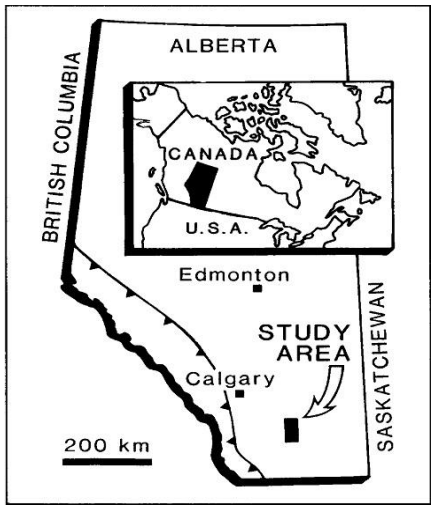

Figure 13. *Index map showing location of study area in the plain of southern Alberta, Canada (From Wood and Hopkins, 1992).*

The Blackfoot is an oil and gas producing field located in the south-east of Strathmore, Alberta, Canada (Figure 13). The 3C-3D seismic survey was acquired over a Lower Cretaceous incised channel filled with sand and plugged shale. The producing formation is cemented channel sand, deposited as incised valley fill sediments in a clastic sequence which unconformable overlie carbonates of Mississippian age. The Glauconitic sandstone is up to 35 m thick and is approximately 1550 m below surface in the Blackfoot area. The average

porosity is near 18% in the producing sandstone and cumulative production throughout southern Alberta exceeds 200 million bbl and 400 billion ft^3 of gas (Margrave et al, 1998).

Data Set Used in the Study

The Blackfoot 3C-3D seismic survey was acquired near Strathmore, Alberta, Canada in 1995 (Stewart et al., 1996). The resulting 3-C data were processed for both P-P and P-S primary reflections to produce two independent 3-D migrated volumes. Final signal bandwidths were 10-80 Hz for P-P and 10-40 Hz for P-S. The subset we use in this study consists of 119 lines and 81 crosslines. The bin size is 30x30 m and offsets ranged from 300 to 1700 m with 11 wells in the covered area. Several published works have discussed these dataset's processing, interpretation (Dufour et al., 1998, 2002, Margrave et al., 1998, Stewart et al., 1996, Pendrel et al, 1998, Swisi and Morozov, 2009).

Methodology

In this study, Short Window Fourier Transform is used to study the spectral decomposition response of Glauconitic sand channel, Blackfoot Alberta. The channel is thin and hard to interpret from seismic images alone (Swisi and Morozov, 2009). Note that the AVO technique has not been widely used for this play, partly because the sinuosity of the channel often requires 3-D data for a satisfactory imaging (Margrave et al. 1998). A strong AVO response conforms to Class III AVO response of Rutherford and Williams (1989) was observed at the top of the porous sandstone in the upper valley exhibiting a low acoustic impedance compared to the encasing shale; whereas the shale in the upper valley had a very different AVO response (Figure 14). Additionally, the products of the rock parameters, incompressibility and rigidity with density were extracted from the result of seismic inversions for P and S -impedances and published by Dufour

et al. (2002), and Swisi and Morozov (2009). All these information help us make a clear image of the channel and pose a great challenge for spectral decomposition as an innovative application to confirm the AVO analyses and inversion results.

For minimizing uncertainty and risk that might be generated from horizons tracking which certainly will affect all further processes, I have selected a geophysically recognizable horizon based on well ties and calibration to well data. I, then, for such careful tracking have invoked Horizoncube, the commercial plugin in OpendTect software (De Groot et al., 2010).

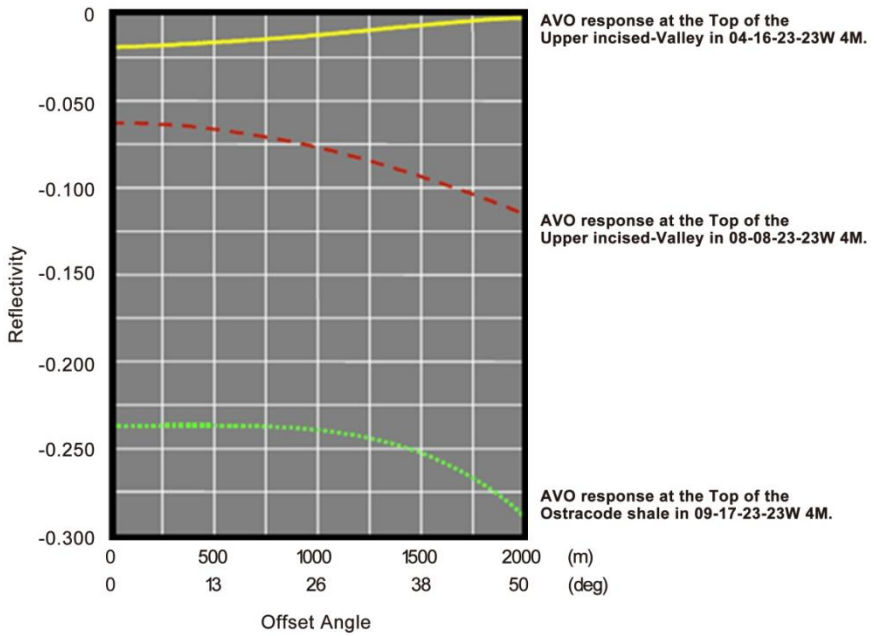

Figure 14. *The AVO response comparison (based on logs) between the upper valley fill (porous sandstone versus shale), as well as with the equivalent regional lithology (Ostracod) (from Dufour et al. 1998).*

The approach currently being adopted for generating the horizon cube involves two main steps. First, a dip "steering cube" is generated which calculates local

dip azimuth at an every sample position within the seismic. The smoothed steering cube is subsequently used to generate a dense set of autotracked horizons that are typically separated by one sample apart on average. This densely tracked horizons mapping technique enables us to generate a set of continuous, chronologically consistent horizons. I then extracted different attributes and perform analysis at the time that the reservoir interval occurred. After that I studied carefully the spectral-decomposition response to different channel fills. Each frequency component was expected to help understand and interpret subtle details about the fluid and the stratigraphic framework of the reservoir.

Results and Discussion

Seismic broadband amplitude analysis showed that the channel's seismic expressions are difficult to discern. Moreover, due to the sinuosity and complexity of the channel, the AVO technique could not be used widely.

Several frequencies were computed for a single horizon. I display the seismic horizon and corresponding isofrequency components at 15, 30 and 45 Hz (Figures 15, 16 and 17).

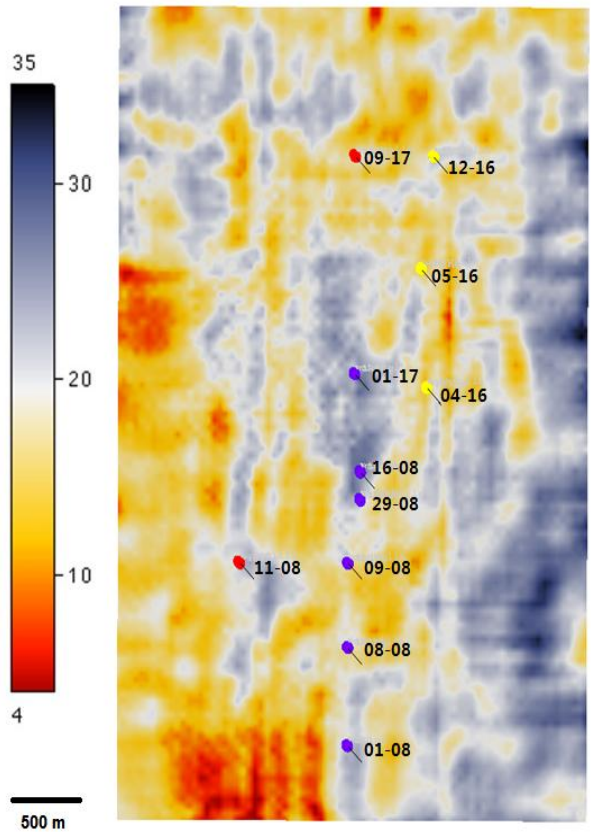

Figure 15. *The spectral amplitude at 15Hz shows some details of the channel. Note that the oil producing wells are in purple, while the dry wells are in yellow. 09-17 and 11-08, the ones in red, are regional wells with gas production from shallower zones.*

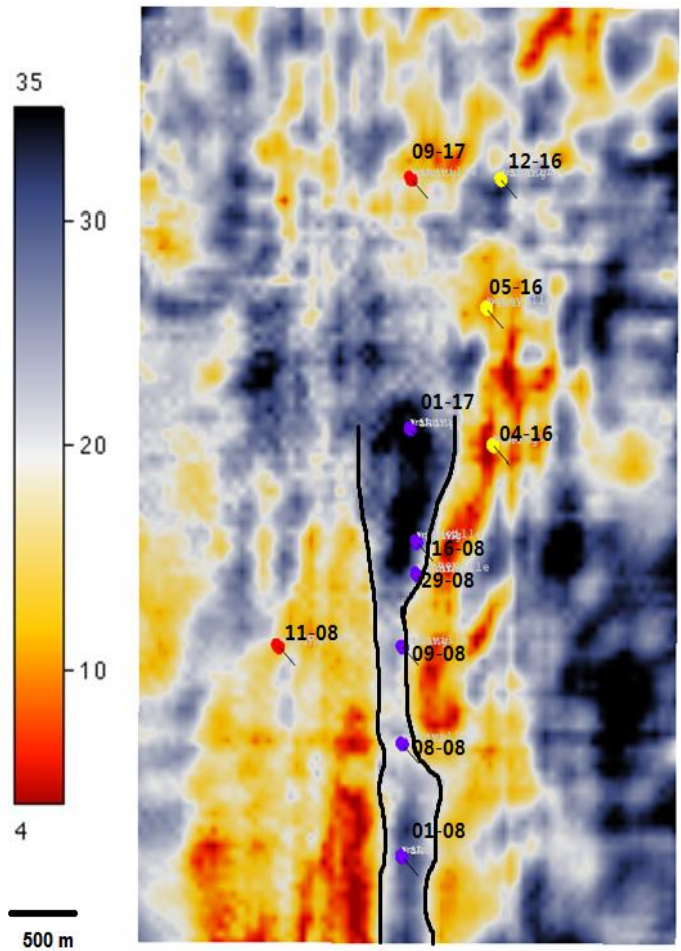

Figure 16. *The spectral amplitude at 30 Hz shows the channel's like structure. Note that the oil wells (purple) are present along the channel area with a high amplitude, while the dry wells (yellow) are beyond the channel with a low amplitude. 09-17 and 11-08 (red) are regional wells with a gas production from shallower zones.*

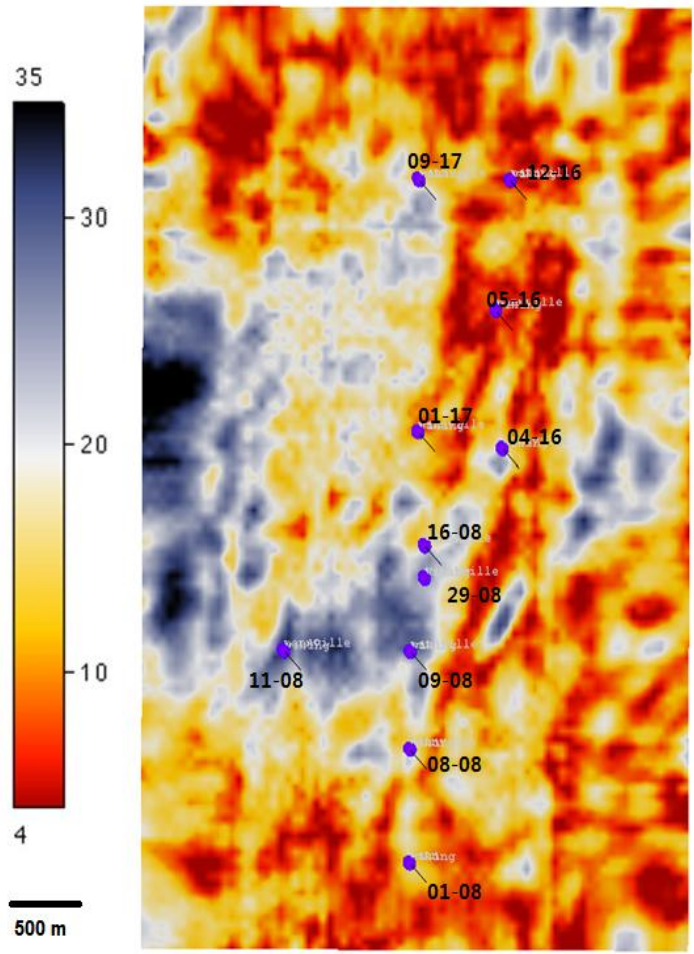

Figure 17. *The spectral amplitude at 45Hz. Note that the channel-like structure disappears at this frequency component. The producing wells are in purple, while the dry wells are in yellow. 09-17 and 11-08 (red) are regional wells with a gas production from shallower zones.*

At 15 Hz the channel is poorly imaged but is clearly visible on a 30Hz spectral component and dims again at 45 Hz, ensuring that 30Hz is closer to the tuning frequency than 15 Hz and 45 Hz are. The anomalous amplitude at 30 Hz can be attributed to the result of both a thin bed tuning and a hydrocarbon charge which is observed only in hydrocarbon bearing sandstones. The hydrocarbon presence

makes the reservoir reflectivity coefficients larger than those in the adjacent non hydrocarbon filled areas, and the thin bed tuning effect of those large reflection coefficients preferentially reflects frequencies higher than 15 Hz and less than 45 Hz, thus, making the sand channel brighter and clearer at 30 Hz than at other frequencies. The difference between the two frequencies was also calculated (Figure 18).

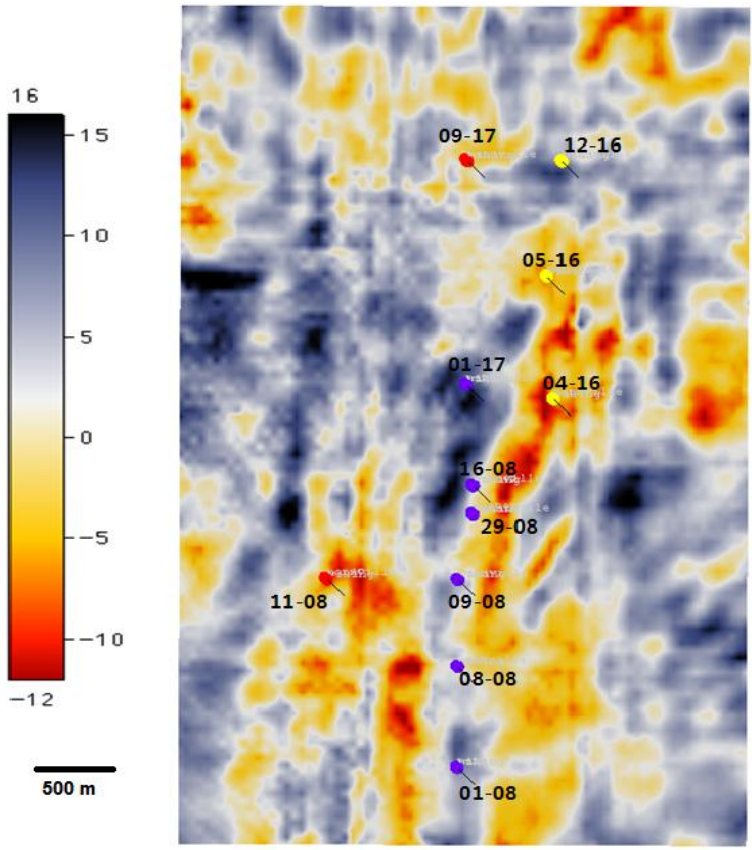

Figure 18. *The spectral amplitude of a high and a low frequency difference. Note that the high frequency contrast is noticeably present along the channel. The producing wells are in purple, while the dry wells are in yellow. 09-17 and 11-08 (red) are regional wells with a gas production from shallower zones.*

The frequency difference horizon slice in Figure 18 shows a high amplitude

trending along the channel compared to areas around the channel. This big difference attributed to the effect of the hydrocarbons presence. In addition, the frequency maps show a different distribution of frequency amplitude within the reservoir. A possible reason for this might be due to a change in the reservoir thickness.

It is important to notice that all these interpretations, derived from spectral decomposition, were consistent with the well information and the limited AVO analyses. A total of 11 wells information within the area covered by the seismic data have been tested. Wells at 01-08, 08-08, 09-08, 29-08, 16-08 and 01-17 (purple) all encountered sandstones at the upper valley level, whereas 04-16, 05-16, and 12-16 (yellow) have only the upper valley shale fill; 09-17and 11-08 (red) are regional wells with gas production from shallower zones. Note that well logs Cross-plotting of well 08-08 and 09-17 inferred that the upper valley has distinctive $\lambda\rho$ and $\mu\rho$ responses compared to tight sandstone and shale (Figure 19).

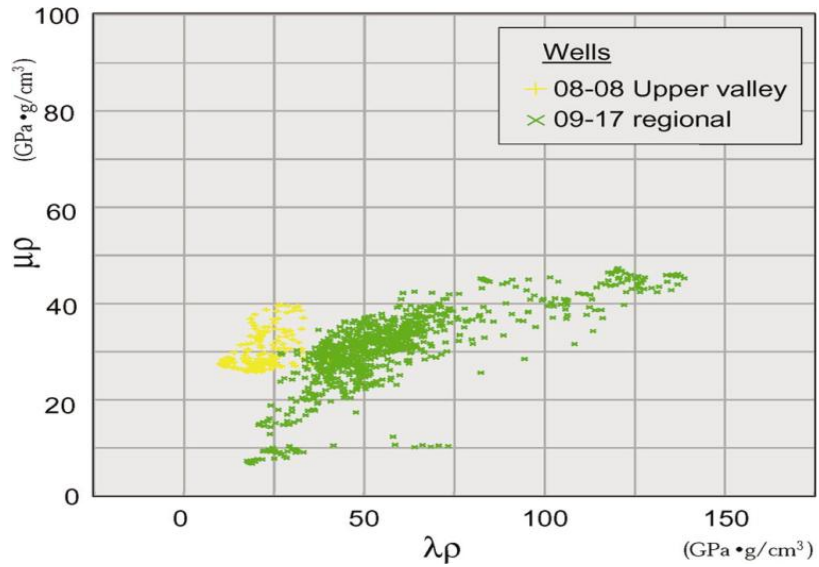

Figure 19. *The crossplot $\lambda\rho$ versus $\mu\rho$ of well 09-17 regional lithologies and well 08-08 upper valley (from Dufour et al., 2002).*

Thus, Dufour et al. (2002) proposed an explanation for that to be due to the fact that porous sandstone in well 08-08 is more compressible (lower $\lambda\rho$) than tight sandstones and more rigid (higher $\mu\rho$) than shales in 09-17. They followed this conclusion by AVO inversion that had indicated the presence of the porous sandstone within the Glauconitic incised-valley system in agreement with the well data information. We notice that the well 09-17 that was ambiguous and challenging in seismic imaging and post stack inversion discussed in Swisi and Morozov (2009) due to the low acoustic impedance response that is similar to the sandstone channel, could be easily differentiated using the AVO inversion and the spectral decomposition.

From Figure 20, it is clear that all the oil producing wells (in purple) found inside the mapped channel, while dry wells lie outside the channel with a low amplitude, except one well (12-16) exhibiting a high anomaly quite similar to the oil wells. The frequency map also indicates a possible reason for this dry well anomaly which is most likely to be associated with a tuning effect. Moreover, amplitude changes have been noticed and thought to be a probable indication of a depositional variation that separates this well from the others and explains why the well does not encounter an oil bearing sandstone.

Although this work presents a successful use of the spectral decomposition and highlights its capacity and simplicity over other relatively complex processes, without the assistance of other sources of information (geology, reservoir engineering, inversion, etc.) the technique does have a limited success in addressing some seismic targets. This is due to the fact that the strata of different lithology and thickness display different spectrum features in the frequency domain, in addition to various factors that may affect the frequency spectrum recorded. Thus, this can generate some difficulties in tuning the optimum frequencies that have the potential to image the desired target through

only the repeated experiments and experience rule. However, there are other more complex techniques, developed mainly to overcome these limitations and to deal with more complex situations and to recognize oil and gas reservoirs when there is few or no prior available information (see Maoshan et al.,2010 and Zhang et al., 2009).

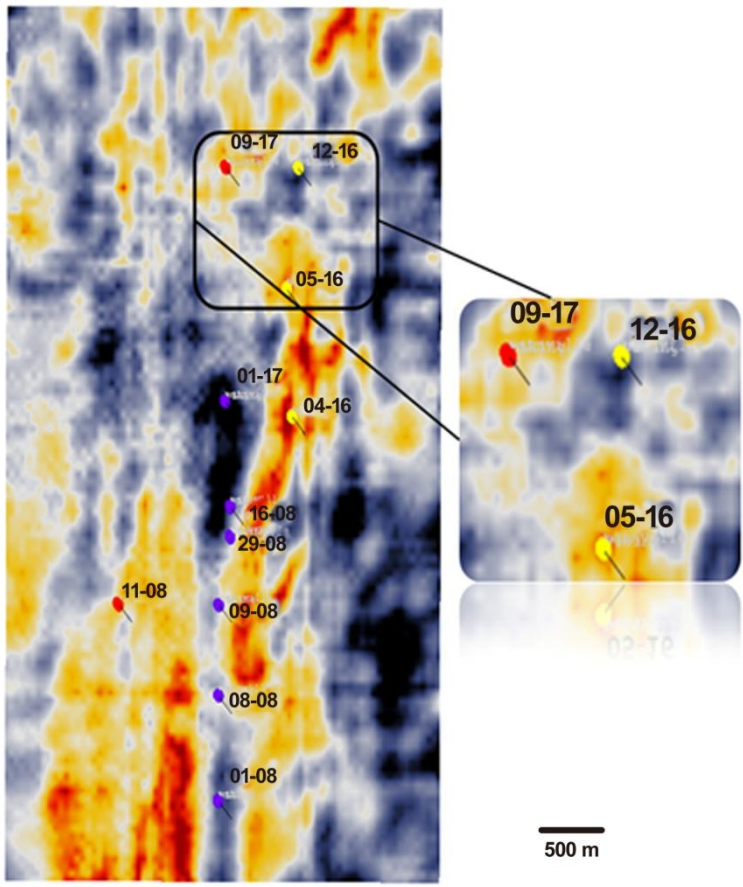

Figure 20. *The 30Hz spectral amplitude and the magnified view of the frequency amplitude behavior around the well 12-16. The change was interpreted as a depositional variation separating this dry well from the oil channel. The producing wells are in purple, while the dry wells are in yellow. 09-17 and 11-08 (red) are regional wells with gas production from shallower zones.*

The study has focused on the spectral decomposition response of the glauconitic channel, southern Canada; and compares it to results inferred from AVO analyses and inversion studies. It is important to note that the spectral decomposition on its own did not characterize the reservoir channel. It is, indeed, the way it has been applied, through creating a very densely picked horizons cube, selecting a recognizable reference horizon close to the channel and targeting the channel interval from the this horizon, that also played a key role in the process. Interestingly, the resulted images confirm the AVO analysis and inversion results and go further by differentiating the producing wells from the dry wells where P wave contrast was not sufficient for a reliable discrimination.

4.9 Conclusion

The seismic attributes proved to be a very powerful tool in extracting subtle information about geologic formations expressions hidden in seismic data.

Some interesting case studies show that seismic attributes play a key role in delivering some vital stratigraphic features that seismic data fails to provide.

The seismic attributes once are well understood and best integrated with other data (e.g. geology, reservoir engineering, etc.), can address very complicated situations and deliver vital information about complex formations.

It is worth emphasizing that just the way one uses the seismic attribute and the tools he incorporates in the interpretation can make a difference and lead to extract key information that cannot be extracted otherwise.

References

[1] Alexander, C., S., Rumelhart, L., M., Raposo, A., and Dominey, J., 2001. The Plutonio discovery, Block 18, Angola-A 3-D visualization and multiattribute approach to exploration success. The Leading Edge, 20, 1393-1400. Amplitude Versus Offset Data: 56th SEG Expanded Abstracts, 332-334.

[2] Avseth, P., Flesche, H. and Wijngaarden, A., V,. 2003. AVO classification of lithology and pore fluids constrained by rock physics depth trends. The leading Edge, 22, 10, 1004-1011.

[3] Brown, A., B., 2001. Understanding seismic attributes. Geophysics, 66, 1, 47-48.

[4] Burnett, M. D., Castagna, J., P., Méndez-Hernández, E., Rodríguez, G., Z., García, L., F., Martínez-Vázquez, J., T., Avilés, M., T., and Raúl Vila-Villaseñor, R., 2003. Application of spectral decomposition to gas basins in Mexico. The Leading Edge, 22, 1130-1141.

[5] Burns, S., and Street, K., 2005. Spectral decomposition highlights faults. Hart's E&P, March, http://www.epmag.com/archives/digitalOilField/2135.htm.

[6] Castagna, J. P., and Backus, M. M., Eds., 1993, Offset-Dependent Reflectivity - Theor and Practice of AVO Analysis: Society of Exploration Geophysicists. Tulsa, OK, 348 p.

[7] Castagna, J. P., Sun S. and Siegfried, R. W., 2003. Instantaneous spectral analysis: Detection of low-frequency shadows associated with hydrocarbons. The Leading Edge, 22, 120-127.

[8] Castagna, J., P. and Smith, S., W., 1994. Comparison of AVO indicators: A modeling study. Geophysics, 59, 12, 1849-1855.

[9] Castagna, J., P., and Sun, S., 2006. Comparison of spectral decomposition methods. First break 24, 75-79.

[10] Castagna, J.P., Swan, H.W. & Foster, D.J. 1998. Framework for AVO gradient and intercept interpretation. Geophysics, 63, 948-956.

[11] Chakraborty, A. and Okaya, D., 1995. Frequency-time decomposition of seismic data using wavelet-based methods. Geophysics, 60, 6, 1906-1916.

[12] Chapman, M., Liu, E. and Li, X.Y. 2005. The effects of abnormally high attenuation on AVO signatures. The Leading Edge 24, 1120-1125.

[13] Chapman, M., Liu, E. and Li, X.Y. 2006. The influence of fluid-sensitive dispersion and attenuation on AVO analysis. Geophysical Journal International 167, 89-105.

[14] Chen, G., Matteucci, G., Fahmi, B., and Finn, Ch., 2008. Spectral- decomposition response to reservoir fluids from a deepwater West Africa reservoir. Geophysics, 73, C23-C30.

[15] Chiburis, E. F., 1987, Studies of amplitude versus offset in Saudi Arabia: 57th Ann. Internat. Mtg., Soc. Expl. Geophys, Expanded Abstracts, 614-616.

[16] Chopra, S., and Marfurt, K. J., 2007. Seismic attributes for prospect identification and reservoir characterization. Society of Exploration Geophysicists, Tulsa, OK, 456 p.

[17] Connolly, P., 1999. Elastic impedance. The Leading Edge18, 438-452.

[18] Cooke, D., and Cant, J., 2010. Model-based Seismic Inversion: Comparing deterministic and probabilistic approaches. CSEG RECORDER, 22-39.

[19] Daubechies, I., 1988. Orthonormal bases of compactly supported wavelets. Communication on Pure and Applied Mathematics, 41, 7, 909-996.

[20] De Groot, P., Huck, A., de Bruin, G., Hemstra, N., Bedford, J, 2010. The horizon Cube: a step change in seismic interpretation. The Leading Edge 29, 9, 1048-1055.

[21] Downton, E., J., Russell, B. H., and Lines, L. R., 2000. AVO for managers: pitfalls and solutions. CREWES Research Report. Volume 12, 21p.

[22] Dufour J., Goodway, B., Shook, I. and Andy Edmunds, A., 1998. AVO analysis to extract rock parameters on the Blackfoot 3C-3D seismic data. SEG Expanded Abstracts 174-177.

[23] Dufour, J., Squires, J., Goodway, W.N., Edmunds, A., and Shook, I., 2002. Integrated geological and geophysical interpretation case study, and Lamé rock parameter extractions using AVO analysis on the Blackfoot 3C-3D seismic data, southern Alberta, Canada. Geophysics 67, 27-37.

[24] Farfour, M., Yoon, W., J., and Jo, Y., (2012) Spectral decomposition in illuminating thin sand channel reservoir, Alberta, Canada. Canadian Journal of

Pure and Applied Sciences 6: 1981-1990.

[25] Fatti, J., L., Smith, G., C., Vail, P., J., Strauss, P., J. and Levitt, P., R., 1994. Detection of gas in sandstone reservoirs using AVO analysis: A 3-D seismic case history using the Geostack technique. Geophysics, 59, 1362-1376.

[26] Forrest, M., Roden, R. and Holeywell, R., 2010. Risking seismic amplitude anomaly prospects based on database trends: The Leading Edge, 29, 936-940, http://dx.doi.org/ 10.1190/ 1.3422455.

[27] Gassaway, G. S., 1984, Effects of shallow reflectors on amplitude versus offset (seismic lithology) analysis: 54th Ann. Internat. Mtg., Soc. Expl. Geophys., Expanded Abstracts, 665-669.

[28] Goloshubin, G., Vanschuyver, C., Korneev, V., Silin, D., and Vingalov, V., 2006. Reservoir imaging using low frequencies of seismic reflections. The Leading Edge, 25, 527-531.

[29] Goodway, B., Chen, T., and Downton, J., 1997, Improved AVO fluid detection and lithology discrimination using Lam é petrophysical parameters; " λρ "," μρ", and"λ/μ fluid stack", from P and S inversions. SEG Expanded Abstracts 183-186.

[30] Goupillaud, P., Grossmann, A., and Morlet, J., 1984. Cycle octave and related transforms in seismi signal analysis. Geoexploration, 23, 1, 85-102.

[31] Hampson, D., P., and Russell, B., H., and Cardamone, M., 2004, Uncertainty in AVO- How can we measure it? CSEG Recorder, March, 5-11.

[32] Hampson, D. P., and Russell, B., H., and Bankhead, B., 2005. Simultaneous inversion of pre-stack seismic data, 75th Annual International Meeting of Society of Exploration and Geophysics (Expanded Abstract), Houston, p. 1633-1637.

[33] Han, D- H. and Batzle, M., 2002. Fizz water and low gas-saturated reservoirs. The Leading Edge, 21 (4), 395-398.

[34] Hardage BA, Carr DL, Lancaster D E, Simmons JL, Hamilton DS, Elphick RY, Oliver KL and Johns RA (1996a) 3D seismic imaging and seismic attribute analysis of genetic sequences deposited in low accommodation conditions. Geophysics 61: 1351-1362.

[35] Hardage BA, Simmons JL, Lancaster DE, Elphick RY, Edson RD, and Carr DL

(1996b) Boonsville 3-D Seismic Data Set: The University of Texas at Austin, Bureau of Economic Geology 32p.

[36] Ito, H., DeVilbiss, J., and Nur, A., 1979, Compressional and shear waves in saturated rock during water-steam transition: J. Geophys. Res., 84, 4731-4735.

[37] Loizou, N., Liu, E. and Chapman, M., 2008. AVO analyses and spectral decomposition of seismic data from four wells west of Shetland, UK. Petroleum Geoscience 14, 355-368.

[38] Loizou N, and Chen S, 2012. The application and value of AVO and spectral decomposition for derisking Palaeogene prospects in the UK North Sea. First break 30 6: 55-67.

[39] Mallat, S., 1989. A theory of multi resolution signal decomposition, the wavelet representation. IEEE Transaction on pattern analysis and machine intelligence, 11, 7, 674-693.

[40] Mallat, S., 2009. A wavelet tour of signal processing, 3rd ed.: Academic Press Inc, Burlington, 805p.

[41] Maoshan, C., Zhonghong, W., Hongying, Z. and Haizhen, Z., 2010. Spectral decomposition and derived techniques for clastic reservoir identification and its application. 80th Annual International Meeting of Society of Exploration and Geophysics (Expanded Abstract), Denver, p.1571-1575.

[42] Margrave, G., Lawton, D., and Stewart, R., 1998. Interpreting channel sands with 3C-3D seismic data. The Leading Edge, 17, 509-513.

[43] Miao, X., Todorovio-Marinic, D., and Klatt T., 2007. Enhancing Seismic Insight by Spectral Decomposition, 77th Annual International Meeting of Society of Exploration and Geophysics (Expanded Abstract), San Antonio, p.1437-1441.

[44] Morlet, J., Arens, G., Fourgeau, E., and D., G., 1982. Wave propagation and sampling theory. Geophysics, 47, 2, 203-236.

[45] Odebeatu, E., Zhang, J., Chapman, M., Liu, E. and Li, X.Y. 2006. Application of spectral decomposition to detection of dispersion anomalies associated with gas saturation. The Leading Edge 25(2), 205-210.

[46] Partyka, G., Gridley, J., Lopez, J., A., 1999. Interpretational applications of

spectral decomposition in reservoir characterization. The Leading Edge, 18, 353-360.

[47] Pendrel, J., Robert, R. Stewart R., and Van Riel, P., 1998. Interpreting sand channels from 3C-3D seismic inversions. Presented at 1998 SEG International Convention.

[48] Roksandic, M., M., 1995, On: "3-D seismic imaging and seismic attribute analysis of genetic sequences deposited in low- accommodation conditions" (B. A. Hardage, D. L. Carr, D.E. Lancaster, J. L. Simmons Jr., D. S. Hamilton, R. Y. Elphick, K. L. Oliver, and R. A. Johns, Geophysics, 61, 1351-1362), Geophysics 60, 1585-1587.

[49] Roden, R., Castagna, J., and Jones, G., 2005. The impact of prestack data phase on the AVO interpretation workflow-A case study: The Leading Edge, 24, 890-895. http://dx.doi.org/10.1190/1.2056369.

[50] Ross, C., 2002. Comparison of popular AVO attributes, AVO inversion, and calibrated AVO predictions. The Leading Edge, 21 (03), 244-252.

[51] Rutherford, S.R. and Williams, R.H. 1989. Amplitude-versus-offset variations in gas sands. Geophysics, 54, 680-688.

[52] Sinha, S., Routh, P. S., Anno, P. D. and Castagna, J. P., 2005, Spectral decomposition of seismic data with continuous-wavelet transform. Geophysics 70, P19-P25.

[53] Smith, G. C., and Guidlow, P. M., 1987, Weighted stacking for rock property estimation and detection of gas: Geophys. Prosp., 35, 993-1014.

[54] Stewart, R.R., Ferguson, R., Miller, S.L.M., Gallant, E., Margrave, G.F., 1996, The Blackfoot seismic experiments: Broad-band, 3C-3D, and 3-D VSP surveys: CSEG Recorder, 6, 7-10.

[55] Suarez, Y., Marfurt, J. K., and Falk M., 2008. Seismic attribute-assisted interpretation of channel geometries and infill lithology: A case study of Anadarko Basin Red Fork channels. 78thAnnual International Meeting, Society of Exploration Geophysicists Expanded abstract, 963-967.

[56] Swisi, A. and Morozov, I., B. 2009. Impedance Inversion of Blackfoot 3D Seismic Dataset, CSPG CSEG CWLS Convention, 404-407.

[57] Tsingas, C., and Kanasewich, E. R., 1991, Seismic reflection amplitude versus angle variations over a thermally enhanced oil recovery site: Geophysics, 56, 292-301.

[58] Welsh, A., Brouwer, F.G.C., Wever, A., Flierman, W., 2008. Spectral decomposition of seismic reflection data to detect gas related frequency anomalies. 70th EAGE Conference and Exhibition. Extended abstract, 263-267.

[59] Whitcombe, D. N., Connolly, P. A., Reagan, R. L. and Redshaw, T. C., 2002. Extended elastic impedance for fluid and lithology prediction. Geophysics 67, 63-67.

[60] Wood, J. M. and Hopkins, J. C., 1992. Traps associated with paleo-valleys and interfluves in unconformity bounded sequence: Lower Cretaceous Glauconitic Member, Southern Alberta, Canada. AAPG Bulletin, 76, 6, 904-926.

[61] Xie D, Wood, JR, and Pennington, WD (2004) Quantitative seismic facies analysis for thin-bed reservoirs: a case study of the central Boonsville Field, Fort Worth Basin, North-central Texas. SEG Expanded Abstracts 23: 1484-1487.

[62] Yoon W. J. and Farfour, M., 2012. Spectral decomposition aids AVO analysis in reservoir characterization: A case study of Blackfoot field, Alberta, Canada, Computers & Geosciences. 46: 60-65.

[63] Young, K T., and Tatham, R H., 2007. Fluid discrimination of poststack "bright spots" in the Columbus Basin, offshore Trinidad. The Leading Edge, 1510-1515.

[64] Zhang, J., Chapman, M., Liu, E., Li, X.Y., Wang, S. and Liu, Z., 2007. Fluid detection by spectral decomposition: lessons from numerical, physical modeling and field studies. Expanded Abstracts of the 69th EAGE Meeting.

[65] Zhang, K., Marfurt, K., J., Slatt, R., M. and Guo, Y., 2009. Spectral decomposition illumination of reservoir facies. 79th Annual International Meeting of Society of Exploration and Geophysics (Expanded Abstract), Houston, p. 3515-3519.

[66] Zoeppritz, K., 1919, Erdbebenwellen VIIIB, ON the reflection and propagation of seismic waves: Gottinger Nachrichten, I, 66-84.